Evaluation of soil-reinforcement interface shear band

Amr M. Morsy, Gholam H. Roodi & Jorge G. Zornberg
The University of Texas at Austin, USA

ABSTRACT: Geosynthetic-reinforced soil (GRS) systems have become competent alternatives to many critical structural traditional systems. Many of these systems involve the use of single reinforcement layer (e.g. reinforced pavement systems) or multiple reinforcement layers placed alternatively with compacted soil layers (e.g. reinforced retaining systems). While extensive research has been conducted to understand the behavior of these GRS systems, the identification of the shear band evolving at the soil-reinforcement interface has not been well-addressed yet. Shear band is deemed a key property that controls the behavior of the soil-reinforcement composite and its influence zone. Understanding the shear band evolution is particularly relevant to optimize the use of reinforcement layers and their arrangement in GRS systems. This study involved a number of soil-reinforcement interaction testing setups to assess the evolution of soil-reinforcement interface shear band. These setups include the following: (1) a small-scale pullout equipment with a transparent side. This setup was used to evaluate the boundary effect on the soil-reinforcement behavior at small strain levels representative to many GRS applications; (2) a large-scale direct shear equipment with a transparent side to compare the shear band evolution in a pure interface shear condition. The paper presents the results of an implemented testing program that aimed at identifying the soil-reinforcement shear band.

Keywords: Soil-geosynthetic interaction; Soil-geosynthetic shear band; Soil-geosynthetic load transfer.

1 INTRODUCTION

The interaction of reinforcements with the surrounding soil involves complex shear stress transfer mechanisms, the manifestation of which is a shear band that develops in the vicinity of the reinforcement (e.g. Palmeira 2009). The general shear and punching shear failure mechanisms have been reported to provide upper and lower bounds of experimental pullout test results (Palmeira & Milligan 1989, Jewell 1990). The interface shear component between geogrid surface and soil has been generally estimated considering the surface area of the geogrid and the interface shear strength properties between the soil and geogrid. However, a clear understanding of the interaction between soil and geosynthetics requires insight into the area of backfill materials that is affected by the presence of the geosynthetic, referred to as the zone of geosynthetic influence. Understanding the zone of geosynthetic influence under large displacements may be particularly relevant to designs involving failure conditions, where a shear zone is expected to form around the geosynthetic (e.g., geosynthetic-reinforced retaining structures) (Morsy et al. 2017a, 2017b). Understanding the zone of geosynthetic influence under small displacement may also be relevant to designs involving serviceability and performance under small displacement conditions (e.g., geosynthetic-stabilized roadways). Hence, evaluation of the zone of geosynthetic influence under small displacements will significantly benefit studies focused on the soil-geosynthetic interaction under service conditions (e.g., Roodi and Zornberg 2017; Zornberg et al. 2017).

This research evaluates the soil-geosynthetic interaction by capitalizing on recent technologies that would allow generating information, in significant volumes and unprecedented detail, on deformations due to soil-geosynthetic interaction. A major limitation in previous soil-reinforcement interaction research studies has been that the deformation of the embedded reinforcement and its surrounding soil is not measured directly. This study presents an experimental evaluation that allows mapping of the entire displacement field of reinforcement and its surrounding soil (i.e., the development of soil-reinforcement interface shear band). This will ultimately provide a rich source of information that is needed to develop and calibrate soil-reinforcement load transfer models.

2 BACKGROUND

Failure of frictional materials is often characterized by localized deformations along rupture zones. These zones are often referred to as shear bands. These shear bands can be characterized by certain thicknesses and patterns (Alshibli and Sture 1999), which depends on the type of failure occurs in a soil system. Shear bands can be characterized by the thickness and the geometry of the band. In shear band zone two soil bodies slide in opposite directions creating a plane). Thickness of the shear band is proportional to the magnitude of the shear strain. Beyond failure, shear strains in these bands are generally plastic and accommodate most of the further deformation. Extensive research has been conducted to analyze and quantify the shear band mechanism in soils. This has recently involved geosynthetic-reinforced soil systems (e.g., Zhou et al. 2012).

Several factors may affect the thickness of the shear band. Analytical and experimental studies have been conducted to identify and measure shear band thickness. A major factor influencing the shear band thickness involves soil particle size. By using Cosserat's continuum theory, Muhlhaus and Vardoulakis (1987) theoretically derived that the shear band thickness is proportional to mean particle size (D_{50}). Alshibli and Sture (1999) conducted experimental studies on sand using digital image techniques to measure the shear band thickness and found out that the normalized shear band thickness (t/D_{50}) decreases as grain size increases. Bariether et al. (2008) showed that not only particle size affects the interface friction but also particle roundness contributes to the soil-geosynthetics interface. Therefore, it is expected that the thickness of the shear band will vary significantly in granular and coarse soil particles.

Soil-reinforcement interaction also plays a key role in the development of shear band (Morsy 2017). For instance, Fannin and Raju (1993) showed that textured geomembranes mobilize thicker shear bands than that of smooth geomembranes. In turn, shear band thickness plays a key role on the soil-reinforcement composite interaction (Morsy et al. 2017a, 2017b).

3 EXPERIMENTAL TESTING METHODOLOGY

Soil-reinforcement interface shear band was evaluated by conducting pullout and direct shear tests. In this section, characteristics of the test equipment and instrumentations are described along with the test procedures adopted in the experimental program.

3.1 *Pullout test*

A small-scale pullout setup composed of a steel box with internal dimensions of 300 x 250 x 150 mm (width x length x height) was used. The box had a transparent side wall, which allowed direct visualization of the soil adjacent to the embedded reinforcement layer. The front wall of the box had an aperture of 15 mm through which the geosynthetic specimen was extended out of the box. The internal sides of the box were lined using Mylar sheets to minimize friction. The confined portion of the geosynthetic specimen was 300 x 250 mm (width x length). The box was mounted on a loading frame that was equipped with a roller grip. The unconfined portion of the geosynthetic was attached to the roller grip as shown in Figure 1a.

The confining pressure was applied using compressed air into a bladder built in the box lid. The geosynthetic specimen was pulled out of the box at a displacement rate of 1 mm/min. Additional displacement sensors (linear potentiometers (LPs)) were used to measure displacement in the confined length of the geosynthetic. The LPs were attached to three locations along the geosynthetic confined length using high-duty steel wires.

3.2 *Direct shear test*

A large-scale direct shear equipment was adopted in this study to evaluate the soil-reinforcement interface behavior. This equipment has a square shear box with interior dimensions of 298 x 300 x 400 mm (width x length x height), which is close to the size of the small pullout box. The shear box includes two halves that can slide over each other on two side v-rails. The v-rails allow a 3-mm gap between the two halves to eliminate friction, which may add false resistance. Also, the 3-mm gap was selected so as not to allow soil particles to jam between the two halves during the test and adding false resistance.

Geosynthetic specimen was glued to a smooth wooden board and secured to the bottom half of the box. The box half that contains the soil had two transparent walls. The transparent walls allowed direct visualization of soil movement as test progresses. Backfill material was placed and compacted using a hand tamper in two lifts of 37.5 mm to reach a total height of 75 mm and a unit weight of approximately 1.66 kN/m^3.

Normal pressure was applied by placing dead weights on top of the backfill. Shear force was applied using a pneumatic actuator of 120 kN capacity. An S-type load cell of 45 kN capacity was used to measure the shear load. Consistent with the small pullout test, a 1 mm/min shear displacement rate was adopted. Two linear variable differential transformers (LVDTs) were used to measure horizontal displacement of the box and vertical displacement of the soil during the test.

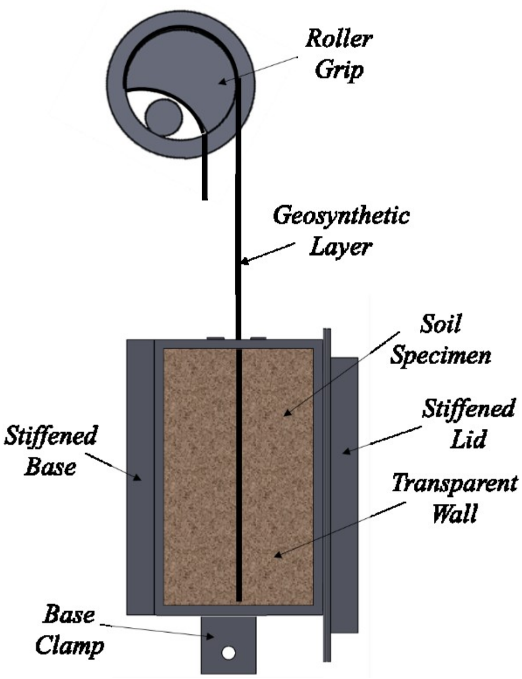

(a)

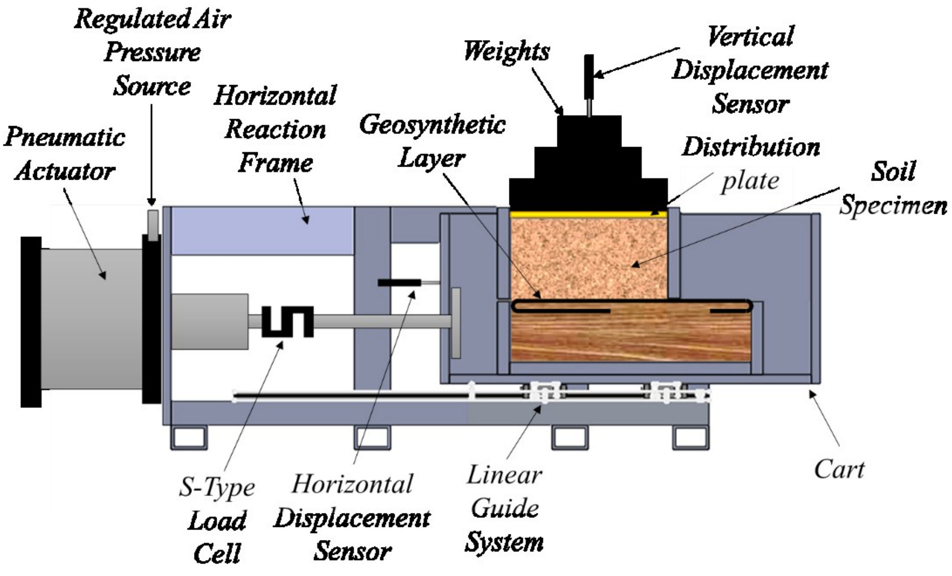

(b)

Figure 1. Testing equipment: (a) pullout equipment; (b) direct shear equipment

4 TESTING MATERIALS

4.1 *Fill material*

The backfill material used in the experimental program involved washed river pea gravel deposited by Colorado River near Austin, Texas. This material is uniformly graded clean gravel classified as GP (poorly graded gravel) according to the Unified Soil Classification System (USCS) and classified as A-1-a according to American Association of State Highway and Transportation Officials (AASHTO) classification (AASHTO M 145). The gravel has gradation that conforms to the standard range of AASHTO No. 8 grain size distribution. This material has sub-rounded to sub-angular particles and consists predominantly of quartz with a trace of other minerals. The grain size of this material ranges approximately from 1 to 13 mm with a mean grain size of 7 mm. The grain size distribution of the material and the AASHTO No.8 gradation bounds are presented in Figure 2. The coefficients of uniformity and curvature are 1.6 and 0.9, respectively. The backfill has a specific gravity of 2.62 and its maximum and minimum dry unit weight of are 16.06 and 17.70 kN/m^3, respectively. That is, the maximum and minimum void ratios are 0.63 and 0.48, respectively.

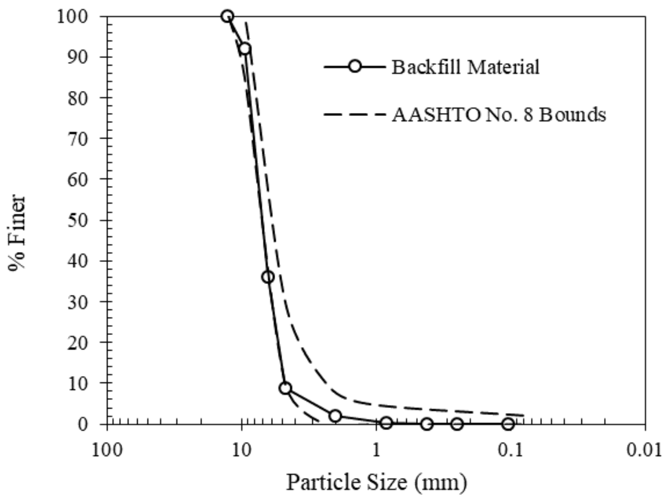

Figure 2. Grain size distribution of backfill material

4.2 *Reinforcement material*

The reinforcement material used in the experimental program was a polypropylene woven geotextile. This geotextile has multi-filament yarns oriented in the rollway direction (i.e., machine direction) and mono-filament yarns oriented in the cross-rollway direction (i.e., cross-machine direction). The rollway direction yarns are connected to each other forming a squeezed rhombic network. The unconfined tensile properties reported by the manufacturer are summarized in Table 1. It was reported that the listed tensile strength properties were obtained in accordance with ASTM D4595. However, these properties are susceptible to variability results from manufacturing, transportation, and storage. In addition, tensile strength and stiffness vary with the strain rate during axial loading.

Table 1. Reinforcement tensile properties

Mechanical Properties	***Minimum Average Roll Value (MARV)***	
	Machine Direction	***Cross-machine Direction***
Ultimate Tensile Strength	70.0 kN/m	70.0 kN/m
Tensile Strength at 2% Strain	14.0 kN/m	19.3 kN/m
Tensile Strength at 5% Strain	35.0 kN/m	39.4 kN/m
Tensile Strength at 10% Strain	70.0 kN/m	70.0 kN/m

5 TESTING PROGRAM

A testing program was implemented to evaluate the interface shear behavior between the baseline fill material (AASHTO No. 8) and the baseline reinforcement type (woven geotextile (GS1)). Table 2 summarizes the characteristics of the tests conducted in this testing program.

Table 2. Interface shear strength testing program

Test Series	*Test*	*Fill Material*	*Normal Stress (kPa)*	*Geosynthetic*
A	Pullout Testing	AASHTO No. 8 (poorly graded gravel)	10.5 21.0 35.0	Woven Geotextile (GS1)
B	Direct Shear Testing	AASHTO No. 8 (poorly graded gravel)	10.5 21.0 35.0	Woven Geotextile (GS1)

6 RESULTS AND ANALYSIS

Figure 3 shows the interface shear stress against the interface shear displacement obtained for both testing methods at different normal stresses. Note that in pullout tests the interface shear displacement was assumed the average displacement of the confined reinforcement portion. Since the reinforcement used has relatively high tensile stiffness, it did not exhibit significant strain in the unconfined zone (290 mm) at the normal stress levels adopted in this study. The interface shear stress for the direct shear tests was calculated by dividing the shear load over the contact area between the reinforcement layer and the soil. On the other hand, the interface shear stress for the pullout tests was calculated by dividing the pullout load over twice the area of the confined reinforcement portion. The area was corrected to account for the decrease in the confined portion as pullout progressed.

It was observed from Figure 3 that the interface shear behavior obtained from the direct shear tests exhibited a peak strength followed by a decay in the strength to a residual strength. On the other hand, the interface shear behavior obtained from the pullout tests showed resistance that increased until reached a plateau without exhibiting a peak. In addition, it was observed that the interface shear strength obtained from the pullout tests was close to the residual strength obtained from the direct shear tests. Overall, the interface strength determined from the direct shear tests was higher than that determined from the pullout tests as shown in Figure 4. However, the interface shear stiffness measured from the pullout tests was greater than that measured from the direct shear tests.

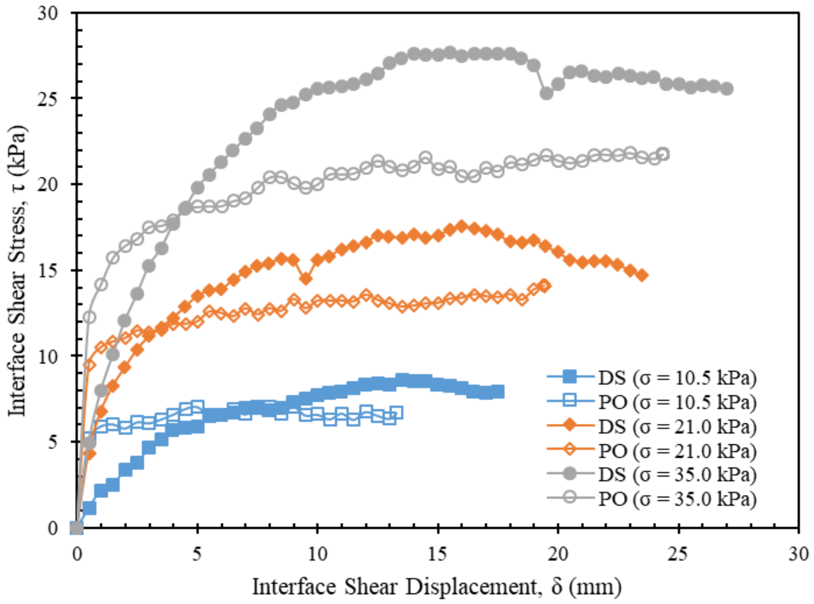

Figure 3. Interface shear stress versus interface shear displacement

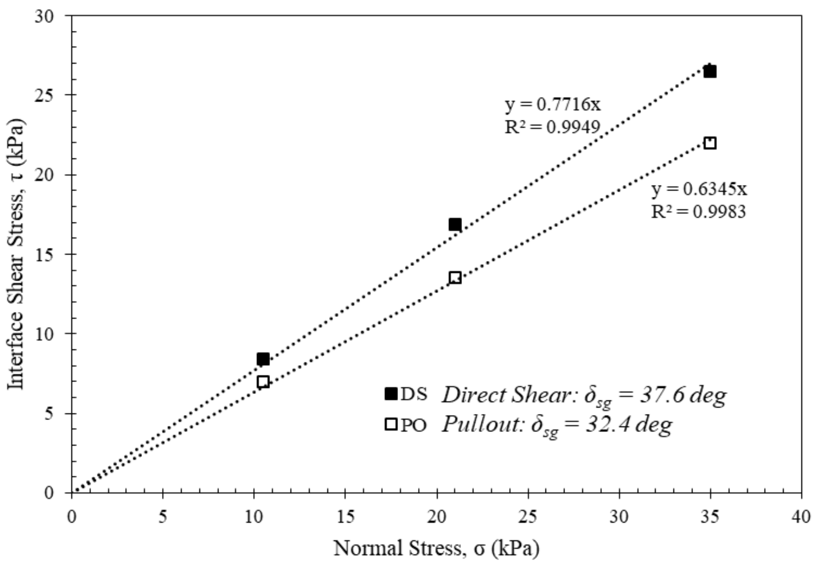

Figure 4. Interface shear failure envelope

Figures 5a and 5b show sample images tethered during direct shear and pullout tests, respectively. The black arrows on the figures denote the direction of the imposed motion on the reinforcement layer. The tethered images were analyzed using Direct Image Correlation (DIC) to measure the soil displacement field. Figure 6 shows the soil displacement at a section located at the center of the soil mass and perpendicular to the reinforcement plane (shown by dotted lines in Figure 5). Specifically, Figures 6a through 6c show the soil displacement at interface shear displacement of 1, 3, and 5 mm, respectively, obtained from both testing methods at different normal stresses.

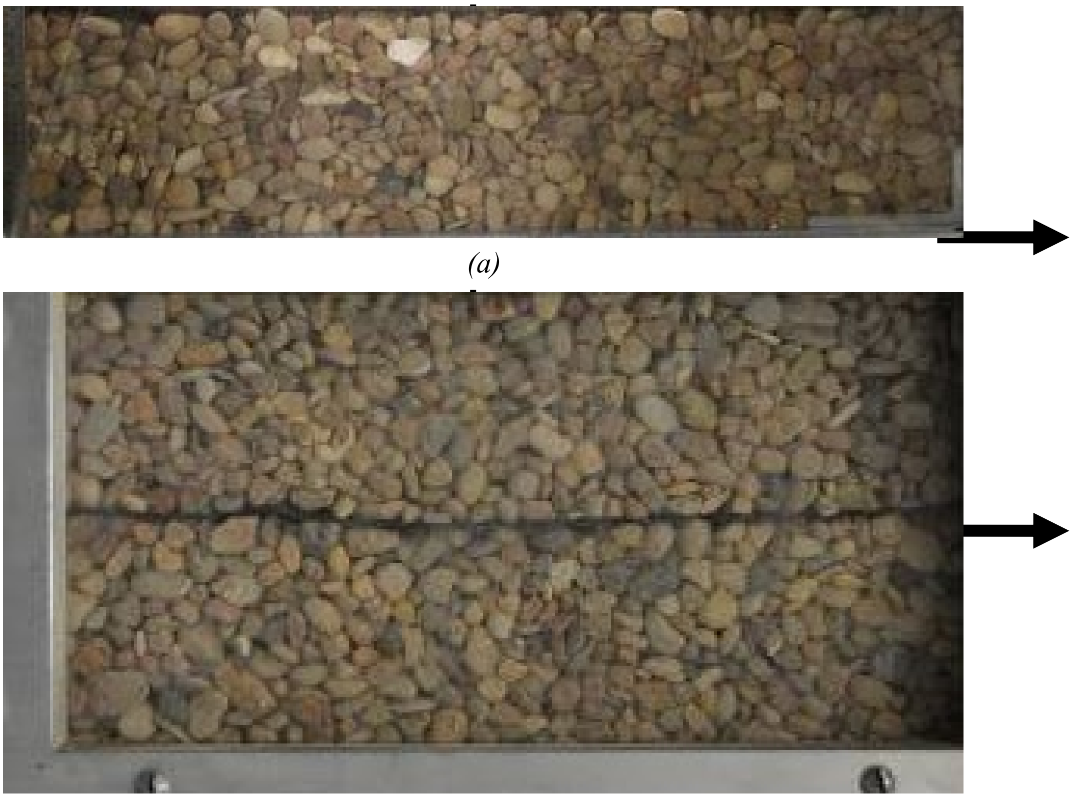

(a)

(b)

Figure 5. Sample frames: (a) direct shear testing; (b) pullout testing (black arrows denote the direction of loading; dotted lines denote cross sections at center of soil mass).

It was observed that the soil displacement increased with the increase in the interface shear displacement. The rate of increase in the displacement magnitude of the soil closer to the reinforcement was higher than that farther from the reinforcement. That is, the reinforcement could convey the load to the adjacent soil more uniformly over a larger zone. As more interface shear, and displacement, was imposed the load began to transfer less uniformly. This observation was clear for results obtained from both testing methods: interface shear stresses mobilized by direct shear load mechanism and interface shear stresses mobilized by pullout load mechanism. However, this was noticed to be higher in results obtained from pullout tests compared to those obtained from direct shear tests. In pullout tests the interaction between the soil and the reinforcement can be higher than that in direct shear tests, especially in case of geogrids and flexile reinforcements. This higher interaction results in smaller magnitudes of soil slippage on reinforcements, which is obvious in Figure 6. It was observed that the magnitude of soil displacement was larger in tests conducted at higher normal stresses except for the soil zones away from the soil-reinforcement interface in pullout tests.

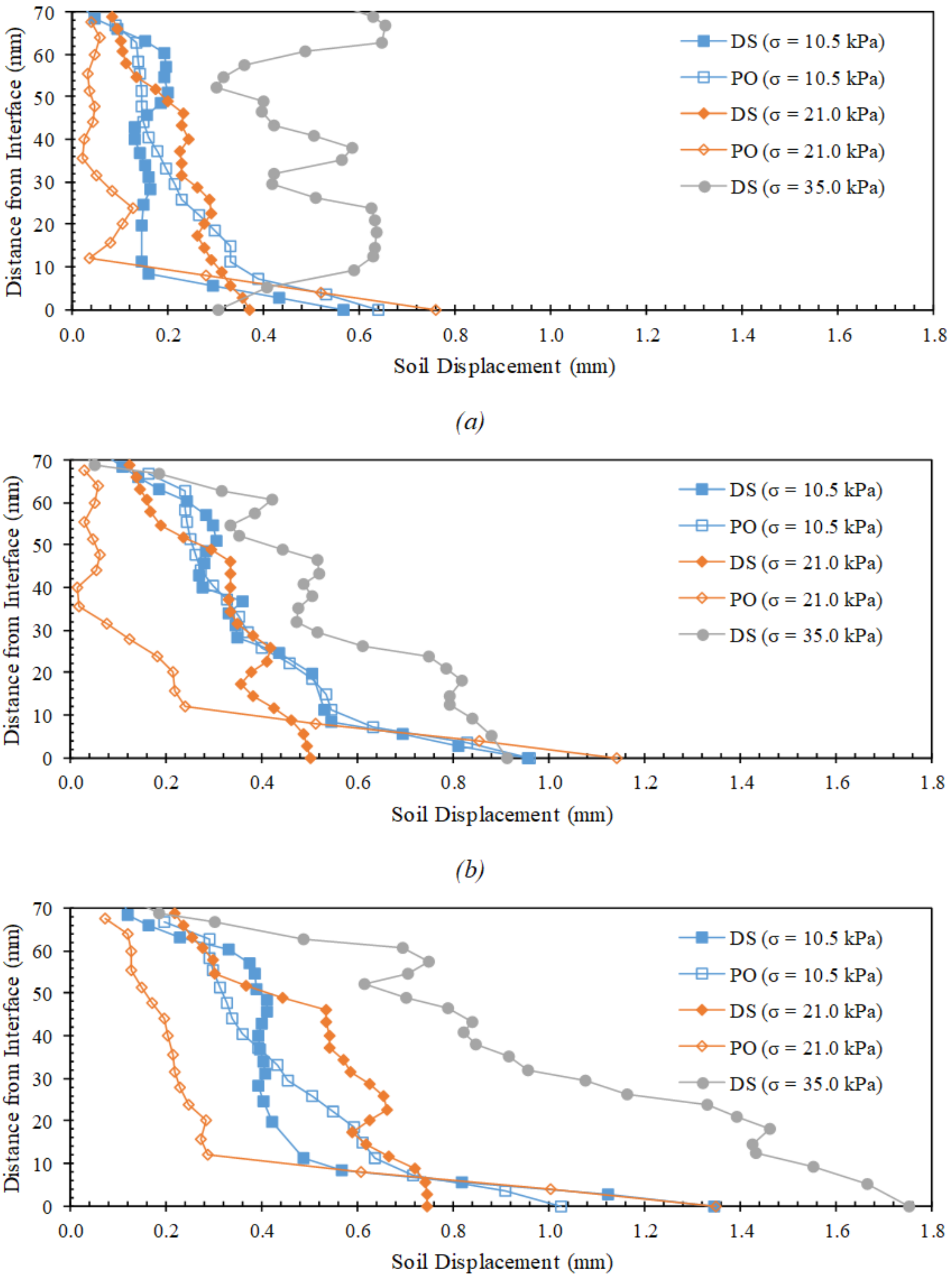

(a)

(b)

(c)

Figure 6. Soil displacement profiles: (a) at interface shear displacement of 1 mm; (b) at interface shear displacement of 3 mm; (c) at interface shear displacement of 5 mm.

7 CONCLUSIONS

This study presents an evaluation of the shear band that forms at soil-reinforcement interfaces in geosynthetic-reinforced soil structures. This evaluation was conducted experimentally adopting two different interface shear loading mechanisms: pullout and direct shear. The paper presents the results of an implemented testing program that employed two devices for the two different mechanisms. The effect of normal stress on the shear band was addressed. In addition, the shear band evolution observed in both mechanisms was compared. The findings of this study summarize as follows:

- Digital imaging is a powerful tool that can provide substantial information in many 2D geotechnical engineering problems.
- Soil-reinforcement interaction is higher in pullout loading mechanism than in direct shear loading mechanism. However, the influence zone that the soil-reinforcement interface has on the adjacent soil is smaller in pullout.
- Soil-slippage at the soil-reinforcement interface is higher in direct shear loading mechanism than that is pullout loading mechanism.
- Soil confinement increases the soil-reinforcement interaction and increases the influence zone the soil-reinforcement interface has on the adjacent soil.

REFERENCES

Alshibli K.A., and Sture, S. (1999), "Sand Shear Band Thickness Measurements by Digital Imaging Techniques," Journal of Computing in Civil Engineering, ASCE, Vol. 2, No. 13, pp.103-109, 1999.

Bareither, C., Edil, T., Benson, C., and Mickelson, D. (2008), "Geological and Physical Factors Affecting the Friction Angle of Compacted Sands," Journal of Geotechnical and Geoenvironmental Engineering, Vol. 134, No. 10, pp. 1476-1489.

Fannin R.J., and Raju, D.M. (1993), "On the Pullout Resistance of Geosynthetics," Can. Geotech. J., Vol. 30, pp. 409-417.

Jewell, R.A. (1990), "Reinforcement Bond Capacity," Geotechnique, Vol. 40, No. 3, pp. 513-518.

Morsy, A.M., Leshchinsky, D., and Zornberg, J.G. (2017a), "Effect of Reinforcement Spacing on the Behavior of Geosynthetic-Reinforced Soil," Proceedings of Geotechnical Frontiers, ASCE, Orlando, Florida, pp. 112-125.

Morsy, A.M., Zornberg, J.G., Christopher, B.R., Leshchinsky, D., Tanyu, B.F., and Han, J. (2017b), "Experimental Approach to Characterize Soil-reinforcement Composite Interaction," Proceedings of the 19th International Conference on Soil Mechanics and Geotechnical Engineering (19th ICSMGE). ISSMGE, Seoul, Korea.

Morsy, A.M. (2017), Evaluation of Soil-Reinforcement Composite Interaction in Geosynthetic-Reinforced Soil Structures, Ph.D. Dissertation, The University of Texas at Austin, Austin, Texas, Austin, Texas. [Draft]

Muhlhaus, H., and Vardoulakis, I. (1987), "The Thickness of Shear Bands in Granular Materials," Geotechnique, Vol. 3, No. 37, pp. 271-283.

Palmeira, E.M. (2009), "Soil-Geosynthetic Interaction: Modelling and Analysis," Geotextiles and Geomembranes, Vol. 27, No. 5, pp. 368-390.

Palmeira, E.M. and Milligan, G.W.E. (1989), "Scale and Other Factors affecting the Results of Pullout Tests of Grids Buried in Sand," Geotechnique, Vol. 39, No. 3, pp. 511-524.

Roodi, G. H., and Zornberg, J.G. (2017), "Stiffness of Soil-Geosynthetic Composite under Small Displacements: II. Experimental Evaluation," Journal of Geotechnical and Geoenvironmental Engineering, ASCE, Vol. 143, No. 10.

Zhou J., Chen, J.F., and Xue, J.F. (2012), "Micro-Mechanism of the Interaction between Sand and Geogrid Transverse Ribs," Geosynthetics International, Vol. 19, No. 6, pp. 426-437.

Zornberg, J.G., Roodi, G.H., and Gupta, R. (2017), "Stiffness of Soil-Geosynthetic Composite under Small Displacements: I. Model Development," Journal of Geotechnical and Geoenvironmental Engineering, ASCE, Vol. 143, No. 10.